Cell. Mol. Biol. (ISSN: 1165-158X)

Journal Homepage: www.cellmolbiol.org

Cellular and Molecular Biology

Original Article

Inhibition of the RIPK1-driven necroptotic pathway protects against hypotensive and tachycardic responses to LPS in a rat model of septic shock

Bahar Tunctan[1*], Sefika Pinar Senol[2], Dilsah Ezgi Yilmaz[1], Omer Bahceli[1], Tuba Kara[3], Muhammed Ahmed-Reda Elosman[1]

[1] *Department of Pharmacology, Faculty of Pharmacy, Mersin University, Mersin, Türkiye*
[2] *Department of Pharmacy Services, Health Services Vocational School, Tarsus University, Tarsus, Mersin, Türkiye*
[3] *Department of Pathology, Faculty of Medicine, Mersin University, Mersin, Türkiye*

Article Info

Article history:

Received: September 14, 2025
Accepted: November 05, 2025
Published: December 31, 2025

Use your device to scan and read the article online

Abstract

Necroptosis, a lytic type of cell death that is dependent on RIPK1-activated RIPK3 and MLKL, has been implicated in the progression of septic shock-related events. However, the role of RIPK1/RIPK3/MLKL necrosome in hemodynamic alterations associated with necroptotic and inflammatory tissue injury due to bacterial infections has not been explored. Therefore, we aimed to investigate whether inhibition of the RIPK1-driven necroptosis by a selective inhibitor of RIPK1, Nec-1s, protects against hypotension and tachycardia associated with necroptotic-, inflammatory-, and injury-related changes induced by bacterial LPS in rats. We also investigated the effects of RIPK1 inhibition on TLR4/TRIF- and caspase-8-related pathways that may contribute to these changes induced by LPS. The MAP and HR values were recorded from the conscious animals using a tail-cuff method. Serum iNOS, HMGB1, MPO, and LDH levels were determined using ELISA kits. The immunoblotting method was used to determine the changes in the expression of proteins related to the TLR4/TRIF- and caspase-8-mediated necroptotic and inflammatory pathways in the TA, RA, PA, and MCA. In the heart, kidney, lung, and brain, histopathological changes were evaluated by the H&E staining method. Expression of RIPK1, RIPK3, MLKL, and HMGB1 proteins in these organs was determined using immunohistochemical staining. Nec-1s prevented LPS-induced hypotension and tachycardia, increased serum iNOS, HMGB1, MPO, and LDH levels as well as expression of unphosphorylated and/or phosphorylated proteins of TLR4/TRIF/RIPK1/RIPK3/MLKL/HMGB1-, TLR4/MyD88/TAK1/IKKβ/NF-κB/iNOS/NO/VASP-, and caspase-8-related pathways in the arterial vasculature, but did not increase RIPK1, RIPK3, and MLKL protein expression induced by LPS in the heart, kidney, and lung tissues. The LPS-induced increase in scores related to histopathological changes in the kidney was attenuated by Nec-1s. These findings suggest that inhibition of the RIPK1-driven necroptosis protects against hypotension and tachycardia, along with arterial and/or renal necroptotic-, inflammatory-, and injury-related changes during septic shock. It also seems that suppression of the TLR4/TRIF- and caspase-8-related pathways may contribute to the beneficial effects of Nec-1s during septic shock.

Keywords: Lipopolysaccharide, Septic shock, Hypotension, Tachycardia, Inflammation, RIPK1-driven necroptosis

1. Introduction

According to the last international consensus (Sepsis-3), sepsis and septic shock are defined as "life-threatening organ dysfunction caused by a dysregulated host response to infection" and "a subset of sepsis in which underlying circulatory and cellular/metabolic abnormalities are profound enough to substantially increase mortality", respectively [1]. It has also been reported that patients with septic shock can be identified with a clinical construct of sepsis with persisting hypotension requiring vasopressors to maintain mean arterial blood pressure (MAP) ≥ 65 mmHg and having a serum lactate level > 2 mmol/L (18 mg/dL), as a result of increased activity of lactate dehydrogenase (LDH), despite adequate volume resuscitation [1]. In addition to LDH, increased myeloperoxidase (MPO) activity is also known to be associated with markers of tissue damage and systemic organ failure during septic shock [2]. The pathogenesis of septic shock is highly complex due to infection, microvascular dysfunction, hemodynamic disturbances, inflammatory tissue injury, and multiple organ failure (MOF) [1-4]. In addition, multiple interconnections and interactions between signaling pathways during septic shock contribute to the complexity of its pathogenesis. For instance, activity of toll-like receptor (TLR) 4/myeloid differentiation factor (MyD) 88- and TLR4/toll-interleukin (IL)-1 receptor domain-containing adapter-inducing interferon-β (TRIF)-dependent pathways in response to the lipid A part of bacterial lipopolysaccharide (LPS) (also

* Corresponding author.
E-mail address: btunctan@mersin.edu.tr (B. Tunctan).
Doi: http://dx.doi.org/10.14715/cmb/2025.71.12.8

known as endotoxin) is increased. The increased activity of these pathways triggered by LPS results in not only increased production of vasodilator/pro-inflammatory mediators but also decreased vasoconstrictor/antiinflammatory mediator formation contributes to the pathogenesis of septic shock [2-5]. Therefore, LPS-induced septic shock is also called "endotoxic septic shock", "endotoxemic shock", "endotoxic shock", "endotoxin shock", or toxic shock [3,4].

Among the vasodilator mediators, it is now well known that nitric oxide (NO) produced in excessive amounts by inducible NO synthase (iNOS) expressed mainly in endothelial and vascular smooth muscle cells contributes to vascular hyporeactivity, fall in blood pressure, inflammation, tissue injury, organ dysfunction, and high mortality rates that are associated with septic shock [2,4]. Activation of TLR4/MyD88/transforming growth factor beta-activated kinase (TAK) 1/inhibitor of κB kinase (IKK) β/inhibitor of κB-α/nuclear factor (NF)-κB/iNOS/soluble guanylyl cyclase/cyclic guanosine monophosphate (cGMP)/protein kinase G (PKG)/vasodilator-stimulated phosphoprotein (VASP) pathway in vascular smooth muscle cells is reported to mediate vasodilatory effect of NO [6]. iNOS deficiency or pharmacological inhibition of NO overproduction opposes the decreased vascular reactivity, hypotension, and tachycardia seen in septic shock [2,4,5]. In our previous studies, we also provided evidence confirming that activation of the TLR4/MyD88 pathway associated with increased expression/activity of iNOS contributes to not only the LPS-induced decrease in vascular reactivity and MAP, but also increase in heart rate (HR), inflammation, and mortality in rats [7-15].

Necroptosis is one of the lytic types of cell death initiated by numerous pro-inflammatory stimuli that requires the activation of receptor-interacting serine/threonine-protein kinase (RIPK) 1, RIPK3, and mixed lineage kinase domain-like pseudokinase (MLKL) necrosome complex [16-18]. During necroptotic signaling, RIPK1 is activated by stimulation of specialized cell receptors, including TLR4 [19,20]. To give an example of the mechanism of RIPK1-related necroptotic cell death *in vitro* and *in vivo* models of inflammation, stimulation of TLR4 leads to activation of the TRIF/RIPK1/RIPK3/MLKL and TRIF/RIPK1/TAK1/IKK pathways, resulting in increased activity of NF-κB, which ultimately promotes inflammatory gene expression, and induction of necroptosis, respectively [19-21]. In the TLR4/TRIF/RIPK1/RIPK3/MLKL pathway, following the phosphorylation of RIPK1, the necrosome complex is formed between RIPK1, RIPK3, and MLKL [22]. Further activation of MLKL by RIPK3 results in the release of damage-associated molecular patterns (i.e., HMGB1), thereby promoting inflammation [22]. In addition, caspase-8, whose activity increases in necroptosis, regulated through TLRs, is reported to prevent necroptosis mediated by MLKL by the ripoptotic signaling complex, RIPK1/RIPK3 [21,23].

Due to its critical role in inflammation and necroptotic cell death in the vascular tissues and vital organs, RIPK1 is considered a prominent target for septic shock management [20]. Therefore, we tested the hypothesis that inhibition of the RIPK1-driven necroptosis prevents hypotension and tachycardia, along with necroinflammatory- and injury-related changes induced by bacterial LPS not only in the arterial tissues, but also in the heart, kidney, brain, and lung. Necrostatin (Nec)-1s, a selective inhibitor of RIPK1, was used to test this hypothesis. We also investigated the effects of RIPK1 inhibition on TLR4/TRIF- and caspase-8-related pathways that may contribute to the LPS-induced changes. It is expected that this study may contribute to the development of selective RIPK1 inhibitors in ongoing efforts to improve the management of septic shock and prevent mortality due to MOF during bacterial infections.

2. Materials and Methods

2.1. Animals

Adult male Wistar rats weighing 200-250 g, typically around 8-10 weeks old, are widely used laboratory animals to induce septic shock models using bacterial LPS. Therefore, adult male Wistar rats aged 9 to 28 weeks and weighing 250 to 450 g (n=42) were used in the study (Research Center of Experimental Animals, Mersin University, Mersin, Türkiye). The animals were kept under a controlled temperature of 24 °C with 50% humidity and a 12-hour light/dark cycle with free access to water and standard rat chow. All of the experimental protocols were approved by the Mersin University Experimental Animals Local Ethics Committee (Approval date: May 25, 2021; Protocol number: 2021/25). The experiments were performed following the National Institutes of Health Guide for the Care and Use of Laboratory Animals under the supervision of a veterinarian. All efforts were made to minimize animal suffering in this research.

2.2. Induction of septic shock model

The septic shock model was induced by an intraperitoneal (i.p.) injection of LPS (*Escherichia coli* LPS, O111:B4; L4130; Sigma Chemical Co., St. Louis, MO, USA) into healthy rats, as previously described [7-15]. In the literature, there is no information regarding the dose of Nec-1 that might prevent LPS-induced hypotension and tachycardia. Therefore, based on the studies conducted in rats and mice [24-29], these experiments were carried out by injecting Nec-1s into rats at appropriate doses (0.1, 0.3, and 1 mg/kg) in a manner that could yield a cumulative normal curve using quantitative log-dose/response relationships frequently used in pharmacodynamic studies. In the experiments to determine the lowest effective dose of Nec-1s that significantly prevents LPS-induced changes in MAP and HR values without causing mortality, were performed in the following groups: (1) saline (control group), (2) LPS (10 mg/kg) (septic shock group), (3) saline+dimethyl sulfoxide (DMSO) (vehicle control group), (4) saline+Nec-1s (1 mg/kg), (5) LPS+Nec-1s (0.1 mg/kg), (6) LPS+Nec-1s (0.3 mg/kg), and (7) LPS+Nec-1s (1 mg/kg). For the *in vivo* experiments, the sample size (n=6 in each group) was determined based on previous studies investigating the effects of various substances on the decrease in MAP and increase in HR in LPS-induced septic shock models in rats, and also confirmed by power analysis [7-15]. One hour after saline or LPS injection, two groups of rats were treated with DMSO (A1584; Applichem GmbH, Darmstadt, Germany) or Nec-1s (17802; Cell Signaling Technology, Inc., Boston, MA, USA). These agents were injected into rats in a volume of 4 mL/kg. Although these agents may cause pain when administered i.p. without anesthesia, an injection requiring brief immobilization may produce acute stress lasting only seconds. On the other hand, injecting a

single dose of an appropriate volume of isotonic solution using a suitable needle into the peritoneal cavity without anesthesia is widely used in studies on experimental septic shock models in conscious rats. Hence, these agents prepared in appropriate solvents were injected intraperitoneally by experienced researchers within 1-2 seconds using a sterile 26-gauge needle to minimize painless administration. Sterile saline and a 1% (volume/volume) dilution of DMSO (0.01 mg/mL final concentration in saline) were used to dissolve LPS and Nec-1s, respectively. The MAP and HR values were recorded non-invasively before and 1, 2, 3, and 4 hours after injection of saline or LPS from the conscious animals using a volume-pressure tail-cuff method (MAY 9610 Indirect Blood Pressure Recorder System, Commat Ltd., Ankara, Türkiye). Before measurement of these values, the rats were kept in a heated chamber at 37 °C for 30 minutes. Since the values will be recorded via a cuff placed on their tails, the animals must be placed in individual chambers appropriate to their size so that they do not move during the measurement period. To minimize distress, care was taken to ensure that the experiments were conducted in a quiet environment and that the total holding time of the animals was approximately 25 minutes for measurements performed 5 times, with a maximum of 5 minutes for each measurement, before and 1, 2, 3, and 4 hours after saline or LPS injection. Except for the measurement of MAP and HR values, the animals were kept in their cages without any restrictions on water, food, etc. Since the animals could move within the restrainer during the measurements, if this situation lasted longer than 5 minutes and did not allow measurements, they were removed from the restrainer and kept in the heated chamber, and the experiment was continued 5-10 minutes later. Under xylazine (7 mg/kg; 0.35 mL/kg; i.p.)+ketamine (90 mg/kg; 0.9 mL/kg; i.p.) anesthesia 4 hours after the saline or LPS injection, and blood sample from vena cava caudalis, thoracic aorta (TA), renal artery (RA), pulmonary artery (PA), middle cerebral artery (MCA), heart, kidney, brain, and lung were taken from these animals. Euthanasia was carried out by the exsanguination of rats. There were no potential confounding factors during the experiments.

2.3. Preparation of serum and tissue samples

Serum samples were prepared from the blood taken [8]. Cytosolic/nuclear fractions of isolated arteries were prepared using a kit (Nuclear Extraction Kit; 10009277; Cayman Chemical, Ann Arbor, MI, USA) and stored at -80 °C [7,8]. The Coomassie blue method was used to determine the total protein amount in these fractions [8]. The isolated heart, kidney, brain, and lung were stored in formaldehyde solution (10%) for histopathological evaluation and immunohistochemical analysis.

2.4. Determination of serum levels of iNOS, HMGB1, MPO, and LDH

Serum levels of iNOS, HMGB1, MPO, and LDH were determined by the enzyme-linked immunosorbent assay (ELISA) method. Rat iNOS ELISA Kit (201-11-0741; Shanghai Sunred Biological Technology Co., Ltd., Shanghai, China), Rat HMGB1 ELISA Kit (MBS703437; MyBiosource, Inc.; San Diego, CA, USA), Rat MPO ELISA Kit (MBS704859; MyBiosource), and Rat LDH ELISA Kit (MBS269777; MyBioSource) were used to measure serum levels of iNOS, HMGB1, MPO, and LDH, respectively.

2.5. Determination of protein expression by immunoblotting

The immunoblotting method was used to determine the changes in the expression of proteins related to the TLR4/TRIF- and caspase-8-mediated necroptotic and inflammatory pathways in the cytosolic and/or nuclear fractions of isolated TA, RA, PA, and MCA tissues as described previously [7]. Briefly, the samples (15 µg of protein) were subjected to a sodium dodecyl sulfate-polyacrylamide gel (10%) together with a molecular weight marker (RPN 800E; Amersham Life Sciences, Cleveland, OH, USA) and subjected to electrophoresis. Following electrophoresis, the separated proteins were allowed to transfer from the gels to the nitrocellulose membranes. After that, the membranes containing proteins were blocked for 1 h at room temperature using 5% non-fat dry milk in tris-buffered saline containing Tween 20 (TBST). The membranes were then incubated with the primary antibodies in bovine serum albumin (BSA) (A7906; Sigma) (1:1.000 in 5% BSA) overnight at 4 °C: (1) TLR4 monoclonal antibody (25) (sc-293072; Santa Cruz Biotechnology, Santa Cruz, CA, USA); (2) TRIF polyclonal antibody (PA5-106871; Thermo Fisher Scientific Inc., Waltham, MA, USA); (3) RIPK1 polyclonal antibody (ARG40183; Arigo Biolaboratories, Hsinchu City, Taiwan); (4) phosphorylated RIPK1 (p-RIPK1) (serine [Ser]^{166}) monoclonal antibody (ARG55746; Arigo Biolaboratories); (5) RIPK3 polyclonal antibody (PA5-19956; Thermo Fisher); (6) phosphorylated RIPK3 (p-RIPK3) (Ser^{232}) polyclonal antibody (PA5-105701; Thermo Fisher); (7) MLKL polyclonal antibody (PA5-102810; Thermo Fisher); (8) phosphorylated MLKL (p-MLKL) (Ser*358*) polyclonal antibody (PA5-105678; Thermo Fisher); (9) HMGB1 monoclonal antibody (HAP46.5) (sc-135809; Santa Cruz); (10) MyD88 monoclonal antibody (E-11) (sc-74532; Santa Cruz); (11) TAK1 monoclonal antibody (D94D7) (5206S; Cell Signaling); (12) phosphorylated TAK1 (p-TAK1) (Ser^{412}) polyclonal antibody (9339; Cell Signalling); (13) IKKβ monoclonal antibody (D30C6) (8943S; Cell Signaling); (14) phosphorylated IKKβ (p-IKKβ) (Tyrosine [Tyr]^{199}) polyclonal antibody (PA5-104694; Thermo Fisher); (15) NF-κB p65 monoclonal antibody (sc-8008; Santa Cruz); (16) phosphorylated NF-κB p65 (p-NF-κB p65) (Ser^{536}) polyclonal antibody (sc-33020; Santa Cruz); (17) iNOS monoclonal antibody (C-11) (sc-7271; Santa Cruz); (18) VASP monoclonal antibody (A-11) (sc-46668; Santa Cruz); (19) phosphorylated VASP (p-VASP) (Ser^{239}) monoclonal antibody (16C2) (sc-101439; Santa Cruz); (20) caspase-8 monoclonal antibody (1H11) (MA5-15914; Thermo Fisher); (21) phosphorylated caspase-8 (p-caspase-8) (Tyr^{380}) polyclonal antibody (PA5-114556; Thermo Fisher); and (22) α-actin monoclonal antibody (1A4) (sc-32251; Santa Cruz). Subsequently, the membranes were incubated for 1 hour at room temperature using sheep anti-mouse IgG-horseradish peroxidase (RPN4201; Amersham) or goat anti-rabbit IgG-horseradish peroxidase (RPN4301; Amersham) as secondary antibodies in TBST containing 0.1% BSA (1:1.000). The images of the immunoreactive bands visualized using ECL Prime Western Blotting Detection Reagent (RPN2232; Amersham) were captured using a gel imaging system (EC3-CHEMI HR Imaging System; Ultra-Violet Products, UVP, Cambridge, UK). To quan-

tify the relative densities of immunoreactive bands, Image J densitometry analysis software (Image J 1.54r, Wayne Rasband, National Institute of Health, Bethesda, MD, USA) was used. The intensities of immunoreactive bands for specific proteins were calculated as a ratio to that of α-actin. The nuclear-to-cytoplasmic (N/C) protein ratios were also calculated to determine whether Nec-1s affect the LPS-induced changes in the nuclear translocation of these.

2.6. Immunohistochemical analysis

Immunohistochemical studies were conducted to measure the expression of RIPK1, RIPK3, MLKL, and HMGB1 proteins associated with necroptosis in heart, kidney, brain, and lung tissues [30,31]. To apply the indicated antibodies using the immunohistochemical method, 2.5-3 µm thick sections from formalin-fixed paraffin-embedded blocks were taken onto positively charged slides, kept in the oven at 68 °C for 1 hour, and deparaffinized by taking them into xylene. The blocked sections were then incubated with RIPK1, RIPK3, MLKL, and HMGB1 for 2 hours. The binding of antibodies was visualized using 3,3'-diaminobenzidine tetrahydrochloride chromogen. RIPK1, RIPK3, MLKL, and HMGB1 positive cells were examined using light microscopy at 4x, 100x, 200x, and 400x magnification. The number of RIPK1, RIPK3, MLKL, and HMGB1 positive cells was calculated based on the total number of cells examined. For all antibodies, the extent of staining in the entire lesion in the stained section was evaluated. The staining percentage values of the stained cells compared to the cells forming the entire lesion are expressed as 1: <25%, 2: 25-50%, 3: 50-75%, and 4: 75-100%.

2.7. Histopathological evaluation

Histopathological studies were carried out to determine hemorrhage, interstitial edema, vascular congestion, inflammatory cell infiltration, and necroptotic changes in heart, kidney, brain, and lung tissues [30,31]. After fixation with 10% formaldehyde, paraffin-embedded tissue sections (4 µm) were stained with hematoxylin and eosin (H&E). Histopathological changes were determined using a light microscope at 100x and 200x objective magnification to determine the severity of changes in detail by a pathologist who was blinded to the group assignment. For heart tissues, congestion, bleeding, vacuolar change in the cell cytoplasm, neutrophil infiltration between muscle fibers, and striation, atrophy, and necrosis in the muscle fibers were evaluated [30]. For kidney tissues, swelling, vacuolization, effacement, and necrosis, in addition to apoptotic cells in the tubule epithelium, were evaluated [30]. Additionally, renal cast, sinusoidal and capillary congestion, glomerular atrophy, subcapsular exudate, interstitial hemorrhage, as well as interstitial, intravascular, and intratubular neutrophil-dominated inflammation have been noted. For brain tissues, edema, enlarged perivascular spaces, neural swelling, pale staining cell cytoplasms, nuclear vacuolization, bleeding, and hyperemia were evaluated [30]. For lung tissues, the presence of leukocytes in the interstitial and alveolar spaces, proteinaceous debris filling the air spaces, the presence of hyaline membranes, and alveolar septal thickening were evaluated [30,31]. The evaluated changes were scored between 0-4 points: 0 points were evaluated as no damage, 1 point as slight damage, 2 points as moderate damage, 3 points as serious damage, and 4 points as very serious damage.

2.8. Statistical analysis

Data are expressed as means ± standard error of means (SEM). For data normally or not normally distributed, parametric or nonparametric statistical analysis was conducted using a one-way analysis of variance followed by Tukey's test for multiple comparisons or Kruskal-Wallis test followed by Dunn's test, respectively, to determine differences from the saline- or LPS-treated groups. GraphPad Prism 10 version 10.0.3 (275) (GraphPad Software, San Diego, California, USA) was used to perform statistical analysis and generate the figures. A P value < 0.05 was considered to be statistically significant. No notable outliers or inconsistencies were observed in the data.

3. Results

3.1. Effect of Nec-1s on LPS-induced hypotension and tachycardia

To determine the effects of RIPK1 inhibition on LPS-induced hypotension and tachycardia, MAP and HR values of saline-, LPS-, and/or Nec-1s-injected rats were measured. As shown in Figure 1, LPS-injected rats presented a progressive drop in MAP values associated with increased HR when compared with those in the control group (P<0.05). MAP was reduced by 46 mmHg and HR increased by 70 beats/minute (bpm) 4 hours after LPS injection into the rats (P<0.05). Nec-1s administered at 1 mg/kg dose restored the MAP and HR values at 1, 2, and 3 hours after its injection into septic rats ($p < 0.05$). The fall in MAP and rise in HR values of the rats injected with LPS were not restored by Nec-1s at the doses of 0.1 or 0.3 mg/kg (P>0.05). MAP and HR values in rats injected with DMSO or Nec-1s (1 mg/kg) were not different from the control group (P>0.05). All rats also survived throughout the experiments. Therefore, sera and tissues of rats treated with a 1 mg/kg dose of Nec-1s were used for further experiments.

3.2. Effects of Nec-1s on rise in systemic levels of iNOS, HMGB1, MPO, and LDH in septic rats

The effects of RIPK1 inhibition on serum levels of iNOS, HMGB1, MPO, and LDH of saline-, LPS-, and/or Nec-1s-injected rats were measured as indices for iNOS/NO/VASP pathway-mediated vascular reactivity, hypotension, and tachycardia, RIPK1/RIPK3/MLKL/HMGB1-

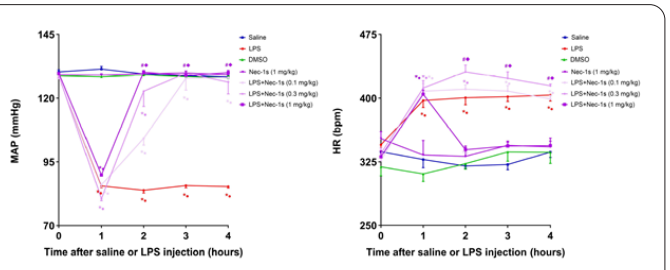

Fig. 1. Effects of Nec-1s on the changes in (A) MAP and (B) HR values induced by LPS in rats. Data are expressed as means ± SEM (n=6 per group). *P<0.05 vs. corresponding value seen in the saline group; #P<0.05 vs. value corresponding to that measured in the LPS-treated group; •P<0.05 vs. time 0 hour value to that measured within a group; ♦P<0.05 vs. time 2 hours value to that measured within a group.

Table 1. Nec-1s prevented the rise in the levels of iNOS, HMGB1, MPO, and LDH measured in the sera 4 hours following injection of saline or LPS into rats.

	iNOS (ng/ml)	HMGB1 ng/ml)	MPO (ng/ml)	LDH (U/l)
Saline	142.80 ± 8.27	10.57 ± 1.57	8.66 ± 0.64	120.60 ± 11.92
LPS	246.70 ± 9.85*	28.83 ± 1.46*	17.54 ± 0.61*	289.90 ± 12.72*
DMSO	149.40 ± 9.41	12.46 ± 1.05	7.91 ± 0.46	113.20 ± 10.94
Nec-1s	137.90 ± 8.58	12.13 ± 1.72	8.18 ± 0.79	133.90 ± 15.15
LPS+Nec-1s	142.10 ± 6.97#	12.19 ± 1.59#	9.73 ± 0.78#	123.20 ± 13.99#

Data are expressed as means ± SEM (n=6 per group). *P<0.05 vs. values measured in the saline-injected group; #P<0.05 vs. values in the LPS-injected group.

mediated necroptosis, MPO-mediated inflammatory tissue injury, and LDH/lactate-mediated cellular damage, during septic shock, respectively. As shown in Table 1, levels of iNOS, HMGB1, MPO, and LDH were found to be increased in the sera of LPS-injected rats when compared with the control group (P<0.05). Nec-1s treatment prevented the LPS-induced increase in serum iNOS, HMGB1, MPO, and LDH levels (P<0.05).

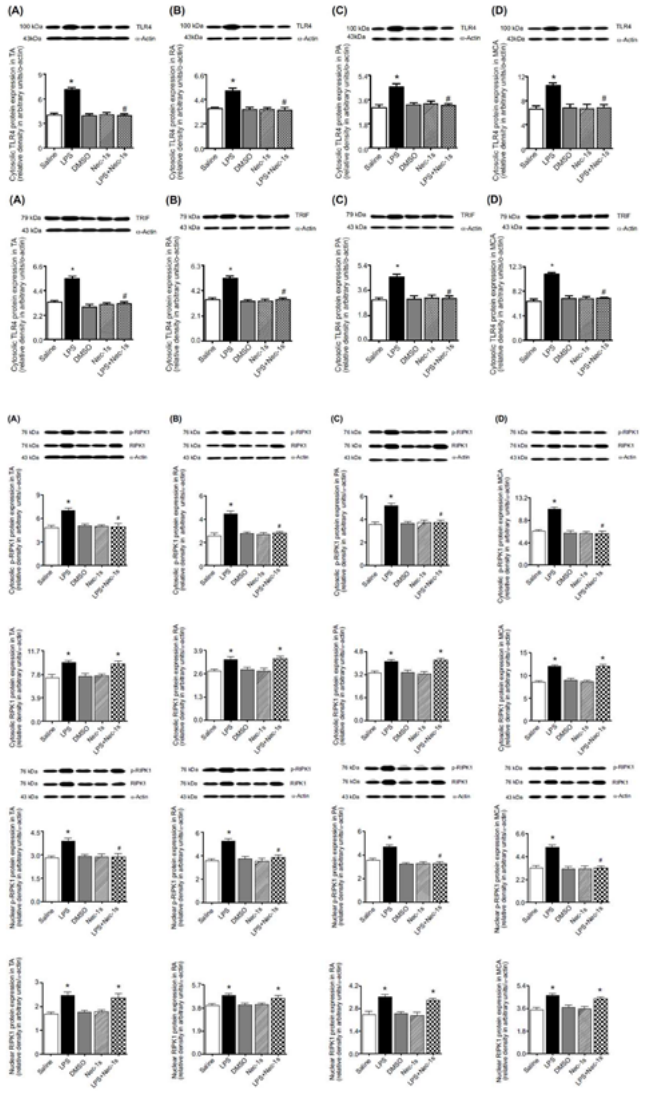

Fig. 2. Effects of Nec-1s on the changes in (A) MAP and (B) HR values induced by LPS in rats. Data are expressed as means ± SEM (n=6 per group). *P<0.05 vs. corresponding value seen in the saline group; #P<0.05 vs. value corresponding to that measured in the LPS-treated group; •P<0.05 vs. time 0 hour value to that measured within a group; ‣P<0.05 vs. time 2 hours value to that measured within a group.

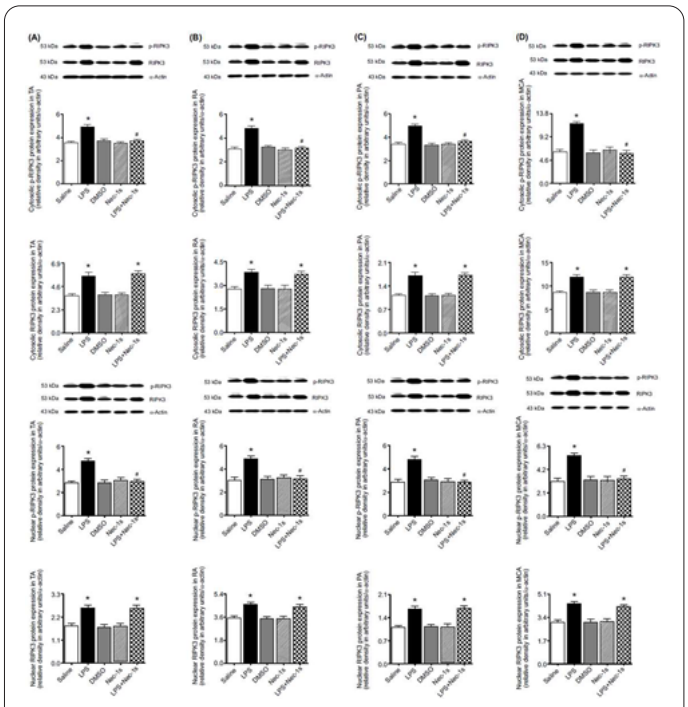

Fig. 2. (continued) Effects of Nec-1s on changes in the expression of phosphorylated and/or unphosphorylated TLR4, TRIF, RIPK1, RIPK3, MLKL, and HMGB1 proteins in the cytosolic and nuclear fractions of (A) TA, (B) RA, (C) PA, and (D) MCA measured 4 hours following injection of saline or LPS into rats. Protein levels in the arterial tissues were measured by immunoblotting. Data represent mean ± SEM (n=4). *P<0.05 vs. values measured in the saline-injected group; #P<0.05 vs. values in the LPS-injected group.

3.3. Effects of Nec-1s on LPS-induced increase in the arterial expression/activity of proteins related to the TLR4/TRIF/RIPK1/RIPK3/MLKL/HMGB1 pathway

To determine the effects of RIPK1 inhibition on the TLR4/TRIF/RIPK1/RIPK3/MLKL/HMGB1 pathway-mediated vascular necroptosis during septic shock, expression of phosphorylated and/or unphosphorylated proteins for TLR4, TRIF, RIPK1, RIPK3, MLKL, and HMGB1 was evaluated in the arterial tissues of saline-, LPS-, and/or Nec-1s-injected rats. LPS injection caused an increase in cytosolic, but not nuclear, TLR4 and/or TRIF protein expression and decreased N/C protein ratio of TRIF in TA (Figure 2A), RA (Figure 2B), PA (Figure 2C), and MCA (Figure 2D) when compared with those in the control group (P<0.05). The increase in cytosolic TLR4 and TRIF expression and decrease in N/C protein ratio of TRIF induced by LPS were prevented by Nec-1s treatment (Figure 2) (P<0.05). Increased expression of RIPK1, p-RIPK1, RIPK3, p-RIPK3, MLKL, and p-MLKL proteins

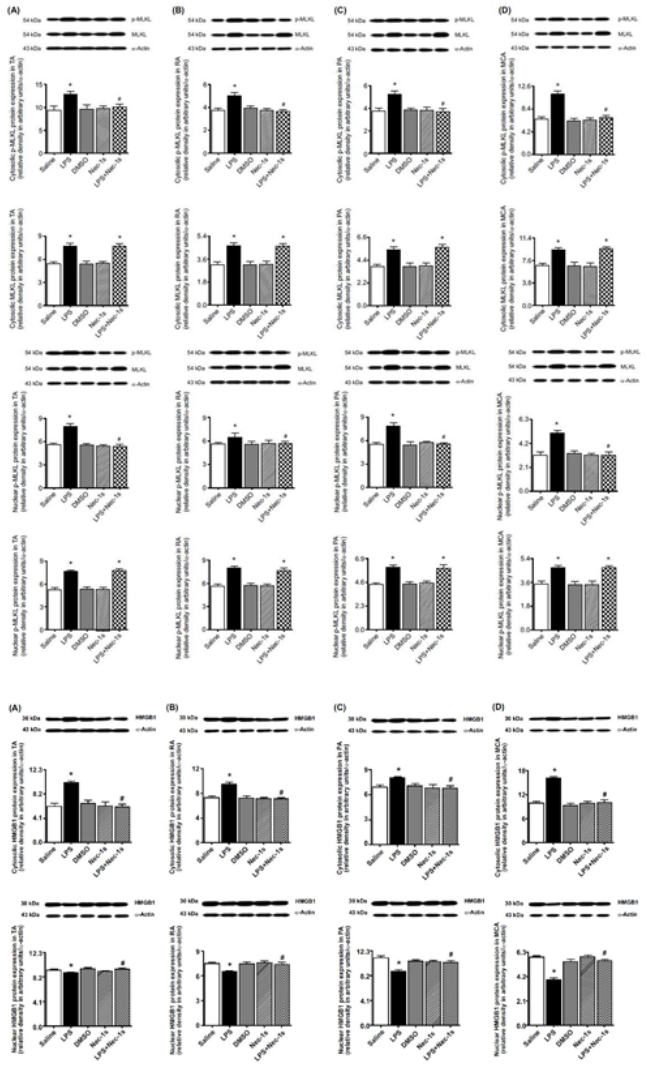

Fig. 2. (continued) Effects of Nec-1s on changes in the expression of phosphorylated and/or unphosphorylated TLR4, TRIF, RIPK1, RIPK3, MLKL, and HMGB1 proteins in the cytosolic and nuclear fractions of (A) TA, (B) RA, (C) PA, and (D) MCA measured 4 hours following injection of saline or LPS into rats. Protein levels in the arterial tissues were measured by immunoblotting. Data represent mean ± SEM (n=4). *P<0.05 vs. values measured in the saline-injected group; #P<0.05 vs. values in the LPS-injected group.

in cytosolic and nuclear fractions and their N/C protein ratios were also observed in the TA (Figure 2A), RA (Figure 2B), PA (Figure 2C), and MCA (Figure 2D) of LPS-injected rats when compared with the control group (P<0.05). The LPS-induced increase in p-RIPK1, p-RIPK3, and p-MLKL, but not RIPK1, RIPK3, and MLKL, expression in both fractions and their N/C protein ratios was prevented by Nec-1s treatment (Figure 2) (P<0.05). Moreover, in the LPS-injected rats, HMGB1 protein expression was increased in cytosolic fractions, while its expression was decreased in nuclear fractions, and a decreased N/C protein ratio was in the TA (Figure 2A), RA (Figure 2B), PA (Figure 2C), and MCA (Figure 2D) when compared with the control group (P<0.05). The LPS-induced changes in HMGB1 expression in these fractions and the decrease in its N/C protein ratio were prevented by Nec-1s treatment (Figure 2) (P<0.05).

3.4. Effects of Nec-1s on LPS-induced increase in the arterial expression/activity of proteins related to the TLR4/MyD88/TAK1/IKKβ/NF-κB/iNOS/NO/VASP pathway

To further determine the effects of RIPK1 inhibition on the TLR4/MyD88/TAK1/IKKβ/NF-κB/iNOS/NO/VASP pathway-mediated vasodilation, hypotension, and subsequent tachycardia during septic shock, expression of phosphorylated and/or unphosphorylated proteins for MyD88, TAK1, IKKβ, NF-κB p65, iNOS, and VASP was also evaluated in the arterial tissues of saline-, LPS-, and/or Nec-1s-injected rats. Injection of LPS resulted in an increase in cytosolic fraction MyD88, p-TAK1, and p-IKKβ protein expression in the TA (Figure 3A), RA (Figure 3B), PA (Figure 3C), and MCA (Figure 3D) when compared with the control group (P<0.05). The LPS-induced increase in cytosolic MyD88 expression was prevented by Nec-1s treatment (Figure 3) (P<0.05). Moreover, the increase in p-TAK1 and IKKβ expression in cytosolic fraction induced by LPS was prevented by Nec-1s treatment (Figure 3) (P<0.05). Protein expression of NF-κB p65, p-NF-κB p65, and iNOS in cytosolic and nuclear fractions and their N/C protein ratios were found to be increased in the TA (Figure 3A), RA (Figure 3B), PA (Figure 3C), and MCA (Figure 3D) of LPS-injected rats when compared with the control group (P<0.05). LPS injection also in-

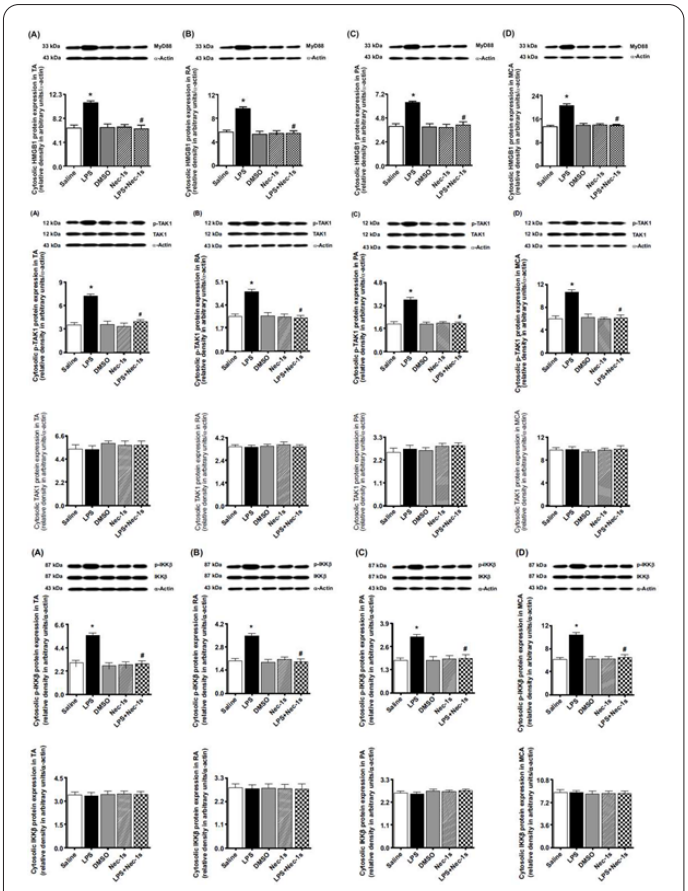

Fig. 3. Effects of Nec-1s on changes in the expression of phosphorylated and/or unphosphorylated MyD88, TAK1, IKKβ, NF-κB p65, iNOS, and VASP proteins in the cytosolic and/or nuclear fractions of (A) TA, (B) RA, (C) PA, and (D) MCA measured 4 hours following injection of saline or LPS into rats. Protein levels in the arterial tissues were measured by immunoblotting. Data represent mean ± SEM (n=4). *P<0.05 vs. values measured in the saline-injected group; #P<0.05 vs. values in the LPS-injected group.

creases cytosolic, but not nuclear, p-VASP protein expression, and decreased their N/C protein ratios in the TA (Figure 3A), RA (Figure 3B), PA (Figure 3C), and MCA (Figure 3D) when compared with the control group (P<0.05). The LPS-induced increase in NF-κB 65, p-NF-κB p65, and iNOS expression in both fractions and their N/C protein ratios were prevented by Nec-1s treatment (Figure 3) (P<0.05). Moreover, the LPS-induced increase in p-VASP expression in both fractions and decrease in their N/C protein ratios were prevented by Nec-1s treatment (Figure 3) (P<0.05).

3.5. Effects of Nec-1s on LPS-induced increase in the arterial expression/activity of caspase-8

To investigate the effects of RIPK1 inhibition on the septic shock-induced vascular necroinflammatory injury, vasodilation, and hypotension by the caspase-8-mediated pathway during bacterial septic shock, expression of unphosphorylated and/or phosphorylated caspase-8 proteins was evaluated in the arterial tissues of saline-, LPS-, and/or Nec-1s-injected rats. Increased cytosolic and nuclear protein expression of caspase-8 and p-caspase-8 and their N/C protein ratios were found in the TA (Figure 4A), RA (Figure 4B), PA (Figure 4C), and MCA (Figure 4D) of LPS-injected rats when compared with the control group (P<0.05). The LPS-induced increase in caspase-8 and p-caspase-8 expression in both fractions and their N/C protein ratios was prevented by Nec-1s treatment (Figure 4) (P<0.05).

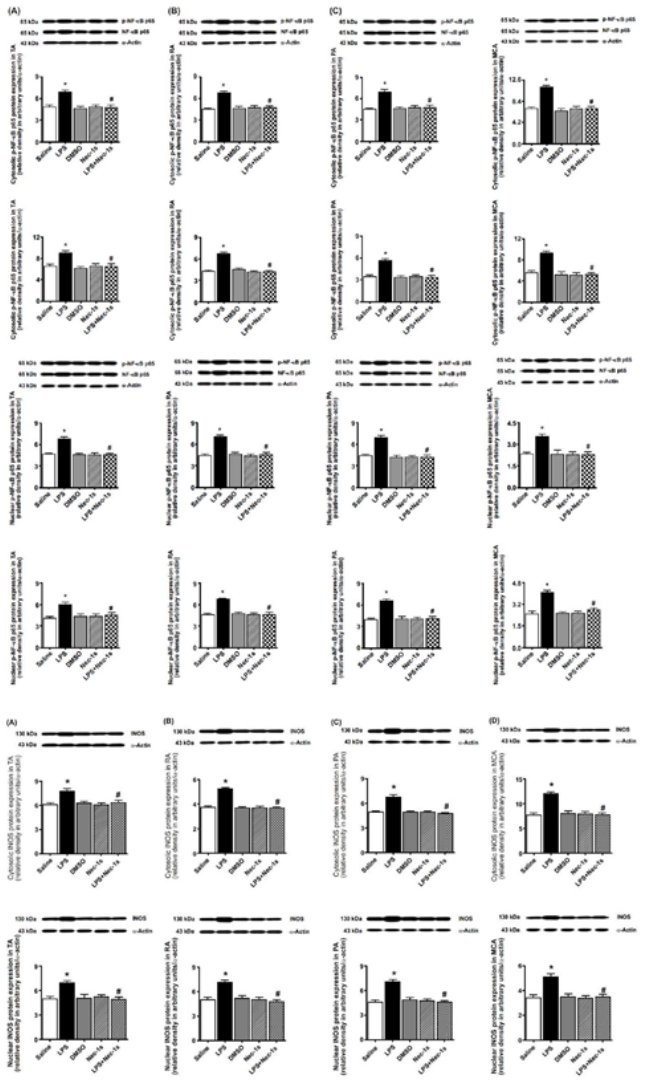

Fig. 3. (continued) Effects of Nec-1s on changes in the expression of phosphorylated and/or unphosphorylated MyD88, TAK1, IKKβ, NF-κB p65, iNOS, and VASP proteins in the cytosolic and nuclear fractions of (A) TA, (B) RA, (C) PA, and (D) MCA measured 4 hours following injection of saline or LPS into rats. Protein levels in the arterial tissues were measured by immunoblotting. Data represent mean ± SEM (n=4). *P<0.05 vs. values measured in the saline-injected group; #P<0.05 vs. values in the LPS-injected group.

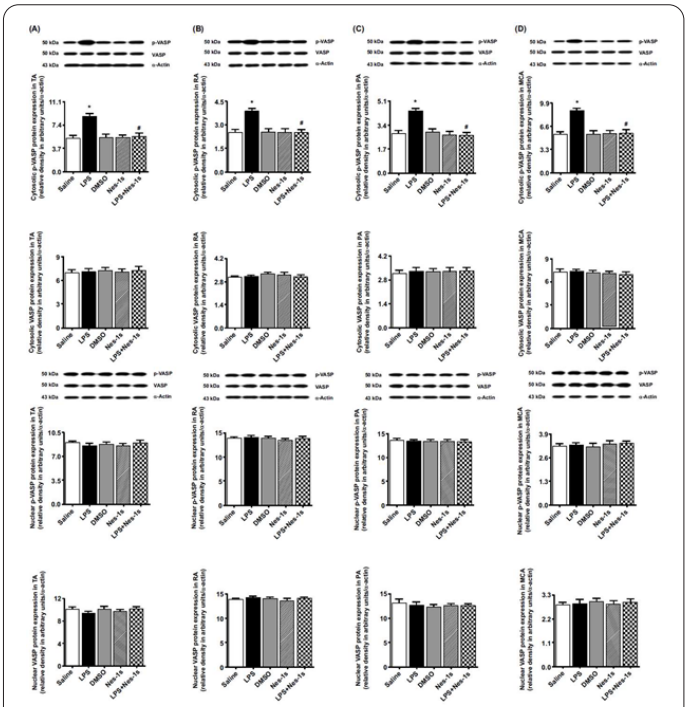

Fig. 3. (continued) Effects of Nec-1s on changes in the expression of phosphorylated and/or unphosphorylated MyD88, TAK1, IKKβ, NF-κB p65, iNOS, and VASP proteins in the cytosolic and nuclear fractions of (A) TA, (B) RA, (C) PA, and (D) MCA measured 4 hours following injection of saline or LPS into rats. Protein levels in the arterial tissues were measured by immunoblotting. Data represent mean ± SEM (n=4). *P<0.05 vs. values measured in the saline-injected group; #P<0.05 vs. values in the LPS-injected group.

3.6. Effects of Nec-1s on LPS-induced expression of RIPK1, RIPK3, MLKL, and HMGB1 proteins in the heart, kidney, brain, and lung tissues

To further explore the involvement of RIPK1/RIPK3/MLKL necrosome in septic shock-induced necroptotic injury and inflammation, expression of RIPK1, RIPK3, MLKL, and HMGB1 proteins was evaluated in the cardiac, renal, cerebral, and pulmonary tissues of saline-, LPS-, and/or Nec-1s-injected rats. LPS injection increased the expression of RIPK3 in the heart (Figure 5A), RIPK1 in the kidney (Figure 5B) and lung (Figure 5D), and MLKL in the kidney (Figure 5B) (P<0.05). The LPS-induced increase in RIPK1, RIPK3, and MLKL expression in the tissues was not prevented by Nec-1s treatment (Figure 5) (P>0.05). It was also observed that expression of RIPK1 in the kidney (Figure 5B), brain (Figure 5C), and lung (Figure 5D), RIPK3 in the kidney (Figure 5B) and lung (Figure 5D), and HMGB1 in the heart (Figure 5A), kidney (Figure 5B), and brain (Figure 5C) of rats administered Nec-1s together with LPS was higher than the values of the control and LPS groups (P<0.05). The expression of RIPK1 in the kidney (Figure 5B) and lung (Figure 5D), RIPK3

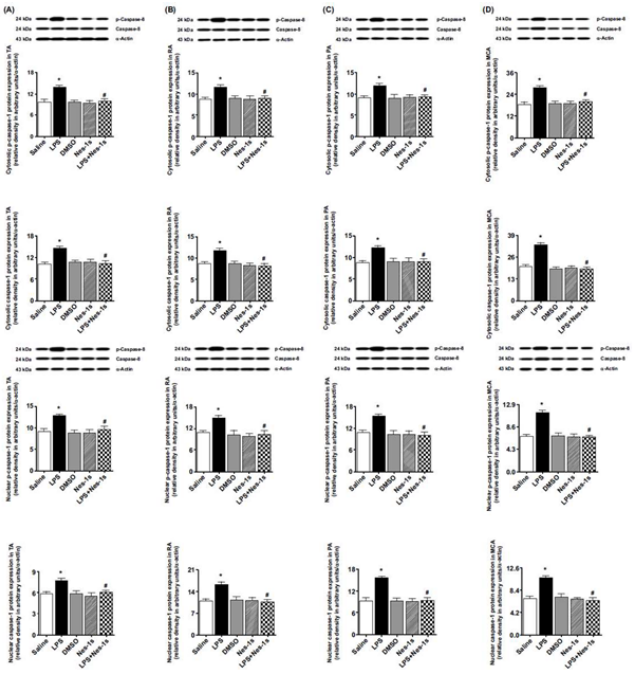

Fig. 4. Nec-1s prevented the increase in the expression of unphosphorylated and p-caspase-8 proteins in the cytosolic and nuclear fractions of (A) TA, (B) RA, (C) PA, and (D) MCA measured 4 hours following injection of saline or LPS into rats. Protein levels in the arterial tissues were measured by immunoblotting. Data represent mean ± SEM (n=4). *P<0.05 vs. values measured in the saline-injected group; #P<0.05 vs. values in the LPS-injected group.

in the heart (Figure 5A), and MLKL and HMGB1 in the lung (Figure 5D) of rats administered DMSO together with saline was higher than the control group (P<0.05). Administration of Nec-1s into saline-treated rats resulted in increased expression of RIPK3 and HMGB1 in the heart (Figure 5A), RIPK1 and MLKL in the kidney (Figure 5B), and HMGB1 in the brain (Figure 5C) (P<0.05).

3.7. Effect of Nec-1s on LPS-induced kidney, heart, brain, and lung injury

To further explore the effects of RIPK1 inhibition on the septic shock-induced inflammatory necroptotic tissue injury, the effects of Nec-1s were evaluated on the histopathological changes in the cardiac, renal, cerebral, and pulmonary tissues of saline-, LPS-, and/or Nec-1s-injected mice. Normal histologic architecture is demonstrated in the heart (Figure 6A), kidney (Figure 6B), brain (Figure 6C), and lung (Figure 6D) tissues of saline-injected rats. Congestion, hemorrhage, vacuolar change in the cell cytoplasm, neutrophil infiltration between muscle fibers and striation, and atrophy and necrosis in muscle fibers observed in heart sections of LPS-injected rats were associated with moderate injury scores (Figure 6A). Swelling, vacuolization, effacement, necrosis, and apoptotic cells in the tubule epithelium observed in kidney sections of LPS-injected rats were associated with serious injury scores (Figure 6B). Edema, enlarged perivascular spaces, neural swelling, pale staining cell cytoplasm, nuclear vacuolization, bleeding, and hyperemia observed in brain sections of LPS-injected rats were associated with mild injury scores (Figure 6C). The presence of leukocytes in the alveolar space, the presence of leukocytes in the interstitial space, the presence of hyaline membranes, proteinaceous debris filling the air spaces, and alveolar septal thickening observed in lung sections of LPS-injected rats were associated with serious injury scores (Figure 6D). The LPS-induced histopathologic changes were attenuated significantly by Nec-1s only in kidney tissue (Figure 6B) (P<0.05). The scores regarding histopathological changes determined in the tissues of rats injected with DMSO and/or Nec-1s together with saline or LPS were higher than the control group values (Figure 6) (P<0.05).

4. Discussion

The results of the study demonstrate that a selective inhibitor of RIPK1 activity, Nec-1s, prevents hypotension and tachycardia associated with necroptotic and inflammatory injury in the arterial and renal tissues of rats with septic shock by not only inhibiting the TLR4/TRIF/RIPK1/RIPK3/MLKL/HMGB1- pathway, but also suppressing the TLR4/MyD88/TAK1/IKKβ/NF-κB/iNOS/NO/VASP-, and caspase-8-related pathways.

During septic shock induced by LPS, NO overpro-

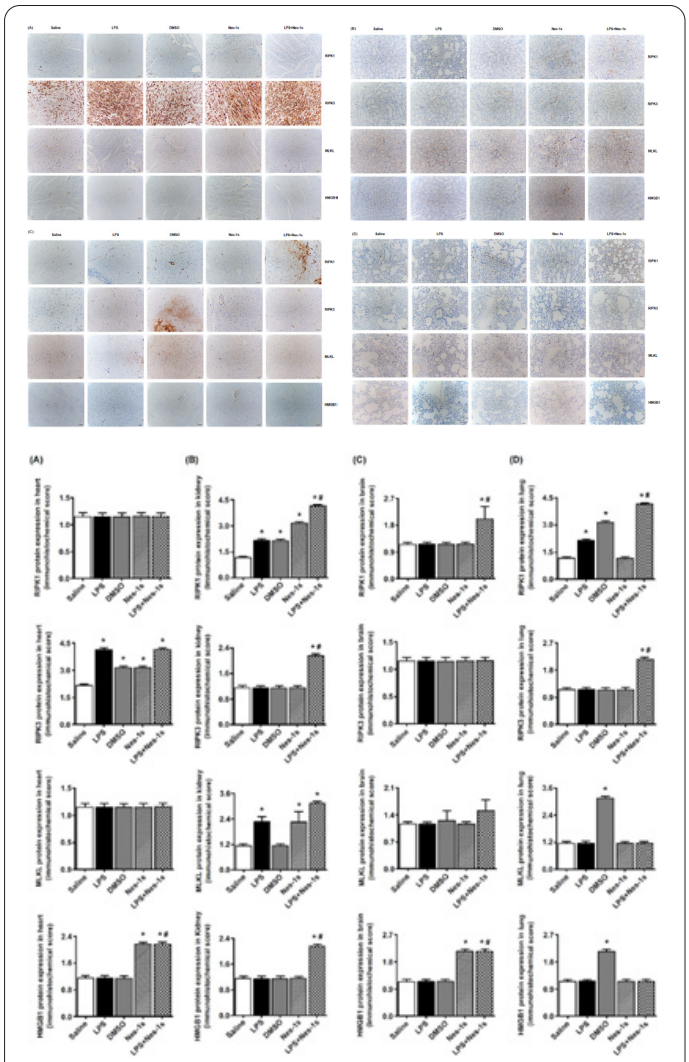

Fig. 5. Nec-1s prevented the increase in RIPK1-, RIPK3-, MLKL-, and HMGB1-positive cell count in (A) heart, (B) kidney, (C) brain, and (D) lung tissues measured 4 hours following injection of saline or LPS into rats. Protein expression was examined by immunohistochemical method (magnification, x200) and scored for the staining percentage values of the stained cells compared to the cells forming the entire lesion. Bar = 100 µm. Data represent mean ± SEM (n=4). *P<0.05 vs. values measured in the saline-injected group; #P<0.05 vs. values in the LPS-injected group.

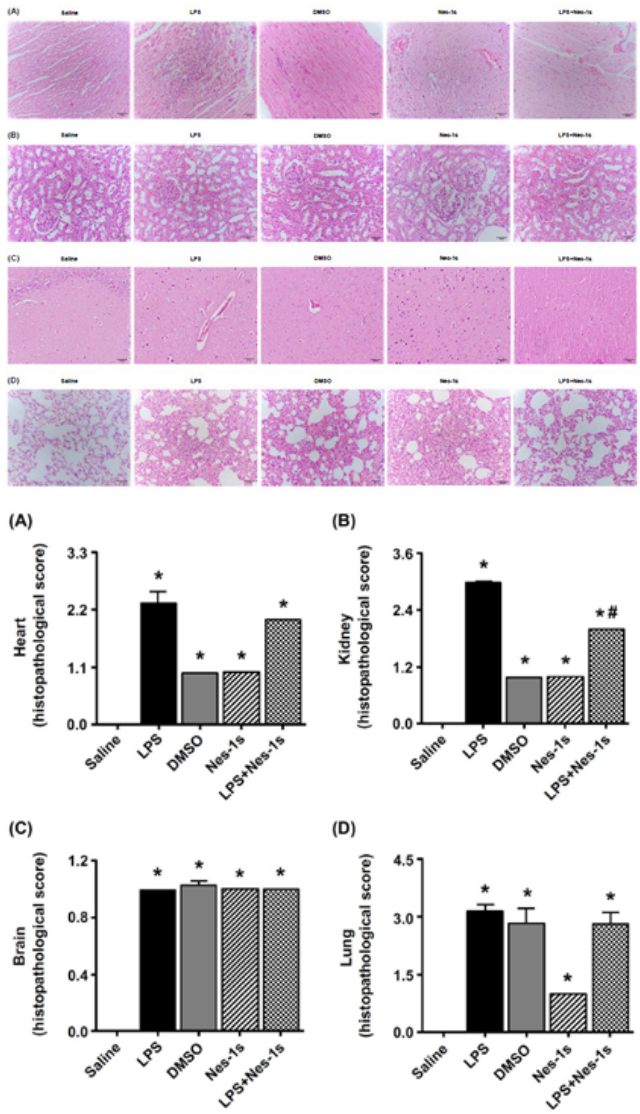

Fig. 6. Effects of Nec-1s on scores determined according to histopathological changes in (A) heart, (B) kidney, (C) brain, and (D) lung tissues measured 4 hours following injection of saline or LPS into rats. Tissue sections were examined for signs of hemorrhage, interstitial edema, vascular congestion, inflammatory cell infiltration, and necrotic changes after H&E staining (magnification, x200) and scored for tissue damage. Bar = 100 µm. Data represent mean ± SEM (n=6). *P<0.05 vs. values measured in the saline-injected group; #P<0.05 vs. values in the LPS-injected group.

duction in the rat arterial tissues through TLR4/MyD88/TAK1/IKKβ/NF-B/iNOS pathway has been reported to be responsible for cGMP-mediated vasodilation by activating PKG and, subsequently, VASP phosphorylation, which results in a decrease in blood pressure and a rise in HR [7,10,11,13,14]. According to the results of studies using iNOS inhibitors, excessive production of iNOS-derived NO during septic shock leads to inflammation, tissue injury, and organ failure [8-10]. Therefore, iNOS is an important therapeutic target due to its importance in the pathogenesis of septic shock. In recent years, compounds such as Nec-1 and Nec1s that selectively target RIPK1-mediated necroptosis [26,32] have also been extensively examined in preclinical studies, especially for use in the prevention and treatment of sepsis and septic shock [20]. Increasing evidence also suggests that necroptosis mediated by RIPK1/RIPK3/MLKL necrosome triggered by activation of the TLR4/TRIF pathway plays a critical role in the pathogenesis of LPS-induced sepsis and septic shock in rodent models [30,32,33]. The results of several studies suggest that Nec-1 has protective effects against LPS-induced systemic inflammatory response [28], sepsis [34], acute kidney [32], and lung [30] injury, as well as neuroinflammation [34] in murine and piglet models. In a study conducted in healthy rats [24], it has been demonstrated that injection of Nec-1 into healthy rats at a dose of 0.8 mg/kg (*intravenous*; i.v.) causes a gradual increase in systolic blood pressure and HR values reaching the peak at 20 min after i.v. drug administration. There are also studies conducted only in mice demonstrating that Nec-1s, a much more selective RIPK1 inhibitor than Nec-1 and possesses improved pharmacological characteristics compared to Nec-1 [26,35], is 0.3 [25], 0.6 [26], 6 [26], or 10 [27] mg/kg (i.p.) or 30 mg/kg (i.v.) [28]. However, MAP and HR were not measured in these studies. It has also been shown that nuclear translocations of RIPK1, RIPK3, and MLKL, which can be prevented by Nec-1, play a role in TNF-α-induced necroptosis in human HT29 colonorectal cell lines [36]. Moreover, Nec-1s is reported to exhibit beneficial effects in necroptosis-related pathological states such as LPS-induced acute systemic inflammatory responses [28,33] and TNF-induced systemic inflammatory response syndrome and mortality [26,33] models in mice. As demonstrated by Szobi et al. [37] in a cardiac I/R model in rats, Nec-1s prevents necroptotic cell death by inhibiting the formation of MLKL oligomers and their subsequent translocation within the plasma membrane. According to the results of these studies, it has been suggested that MLKL deficiency is more important than RIPK1 inactivation or RIP3K deficiency in necroptotic diseases associated with inflammation and tissue damage [33]. On the other hand, according to the results of an *in vitro* study conducted by Kearney et al. [38] on L929 cells, RIPK1 functions to prevent rather than initiate RIPK3-dependent necroptosis. Furthermore, there are studies demonstrating that caspase-8 prevents MLKL-mediated necroptosis by the ripoptotic signaling complex, RIPK1/RIPK3 [21,23]. *In vitro* studies have shown that the RIPK1/RIPK3/Fas-associated death domain/caspase-8 complex formed following LPS stimulation causes pro-inflammatory IL-1β release, which requires the presence of TRIF and RIPK1, and interaction of RIPK3 with TRIF results in the TLR-mediated necroptosis and positive regulation of non-apoptotic caspase-8 [39]. Conversely, it has been suggested that caspase-8 expression and/or activity may also increase as a result of activation of TLR4/TRIF pathway independently from pro-necroptotic RIPK1/RIPK3 and/or TLR4/MyD88 pathways in tissues related to the heart, aorta, and lung in the LPS-induced lung injury [40], endotoxemia [41], sepsis [42], and endotoxic shock [43] rodent models. Results of *in vitro* studies demonstrated that binding of caspase-8 to TRIF and MyD88 following LPS administration contributes to necroptosis [39] mediated by the TLR4/TRIF and TLR4/MyD88 pathways. Moreover, Lemmers et al. [44] demonstrated that caspase-8, whose expression increases through the TLR4/MyD88/IRAK1 pathway in LPS-stimulated mouse B cells, causes an increase in the nuclear translocation of NF-κB, which is activated as a result of its interaction with the IKKα/IKKβ complex. In a study conducted in mouse bone marrow-derived macrophages stimulated with LPS, it was also reported that increased activity of caspase-8 results in increased iNOS

expression and formation of NO [45]. In addition, there are *in vitro* and *in vivo* studies showing that the translocation of RIPK1 [36,46], RIPK3 [36,46], HMGB1 [47], MLKL [36], NF-κB p65 [7,44], iNOS [48], VASP [49], and caspase-8 [50] proteins within the cell is changed in response to various stimuli such as LPS, TNF, I/R, heat stress, and ionomycin. On the other hand, the effects of selective RIPK1 inhibition on the LPS-induced changes in hypotension and tachycardia in addition to the activity of TLR4/TRIF/RIPK1/RIPK3/MLKL/HMGB1-, TLR4/MyD88/TAK1/IKKβ/NF-κB/iNOS/NO/VASP-, and caspase-8-related pathways in the cytosolic and/or nuclear fractions of vascular tissues from septic rats have not been investigated.

The results of our previous studies indicated that systemic administration of LPS into rats results in (1) hypotension and tachycardia [7-15], (2) vascular hyporeactivity in the TA and superior mesenteric artery (SMA) [11], (3) enhanced systemic and/or tissue levels of iNOS/NO [13,14], MPO [10,14], and LDH [14], (4) increased expression and/or activity of MyD88 [7], TAK1 [7], NF-κB p65 [7,12], iNOS [13,14], PKG [13], and VASP [13] in the heart, kidney, and/or TA, and (5) nuclear translocation of NF-κB p65 in the TA, SMA, heart, and kidney [7]. In this study, the reduction in MAP and the rise in HR in response to LPS injection into rats over the 4 hours of the experiment were also observed. Moreover, these changes were associated with (1) elevated serum levels of iNOS, HMGB1, MPO, and LDH, (2) increased expression of TLR4, TRIF, HMGB1, MyD88, NF-κB p65, iNOS, and caspase-8 proteins in addition to the activity of RIPK1, RIPK3, MLKL, TAK1, IKKβ, NF-κB p65, VASP, and caspase-8 in the cytosolic and/or nuclear fractions of TA, RA, PA, and MCA, and (3) increase in the nuclear translocation of unphosphorylated and/or phosphorylated RIPK1, RIPK3, MLKL, MLKL, NF-κB p65, iNOS, and caspase-8 proteins as well as translocation of TRIF, HMGB1, and VASP proteins from the nucleus to the cytoplasm in the vascular tissues of rats with septic shock at 4 hours after LPS administration. Nec-1s prevented the LPS-induced changes, except for increased expression of RIPK1, RIPK3, and MLKL proteins in both fractions. Hence, in agreement with the previous studies, these novel data suggest that Nec-1s, not only by inhibiting RIPK1 activity [26] but also suppressing the TLR4/TRIF/RIPK1/RIPK3/MLKL/HMGB1- and TLR4/MyD88/TAK1/IKKβ/NF-κB/iNOS/NO/VASP-[28,30,32,33] and/or caspase-8-related pathways [39-45] prevent the iNOS-derived NO-mediated hypotension and tachycardia in response to systemic LPS administration in the arterial vasculature in the rat model of septic shock. Our results also suggest that Nec-1s exerts its effects on the changes induced by LPS in the expression of the unphosphorylated and/or phosphorylated proteins involved in these pathways in nuclear and/or cytosolic fractions of vascular tissues of rats. On the other hand, further detailed *in vitro* studies using cells are required to demonstrate the exact cellular sites of action of Nec-1s on the changes triggered by LPS in the subcellular localizations of these signaling proteins and elucidate the molecular mechanisms of functional interactions between them [7,24,37,44,46-50].

In the present study, scores regarding histopathological changes determined in the heart, kidney, brain, and lung tissues also increased 4 hours after administration of LPS into rats. Nec-1s reduced these LPS-induced changes only in kidney tissue. The scores regarding histopathological changes determined in the tissues of rats administered DMSO and/or Nec-1s together with saline or LPS were higher than the control group values. These findings demonstrated that there were changes associated with hemorrhage, interstitial edema, vascular congestion, inflammatory cell infiltration, and necrosis in the heart, kidney, brain, and lung tissues isolated 4 hours after LPS administration into rats. According to our findings, Nec-1s reduces the elevated scores regarding histopathological changes only in the kidney tissue isolated from rats in the LPS-treated group. These findings are consistent with the studies performed in the septic shock model in rats, demonstrating that LPS causes histopathological changes in the heart [51], kidney [32], brain [52], and lung [30,53,54]. Results of *in vivo* studies also demonstrated that Nec-1, another selective RIPK1 inhibitor, reduces or does not prevent LPS-induced kidney and lung injury in mice [28,30,53,54]. Nevertheless, there are no studies investigating the effects of Nec-1s on the histopathological alterations induced by LPS in the heart, kidney, brain, and lung tissues in this septic shock model. Therefore, in this model, it has been shown for the first time in this study that Nec-1s reduces the increase in scores related to LPS-induced histopathological changes only in the kidney tissue, but not in the heart, brain and lung. Also, a matter that needs to be particularly emphasized is that while the MAP and HR values of rats injected with DMSO or Nec-1, compared to the control group, were not significantly changed, the scores regarding histopathological changes in the tissues were found to be higher than the control group values. These findings are also consistent with the results of the *in vivo* studies demonstrating that systemic administration of DMSO or Nec-1 into rats and mice causes histopathological changes similar to kidney and lung injury induced by LPS [30,32,53,54].

In acute lung injury and acute kidney injury in rodents and neonatal sepsis model in rats, there are studies in the literature showing that LPS increases protein expression of HMGB1 in the heart [55] and kidney [56], RIPK1 [57,58], RIPK3 [58], MLKL [57], and HMGB1 [59] in the brain, RIPK1 [30] and HMGB1 [31] in the lung. Additionally, in the neonatal sepsis model in rats and acute lung injury model in mice, it has also been reported that Nec-1 prevents the LPS-induced increase in the expression of RIPK1 [30,57,58], RIPK3 [30,58], and MLKL [57] in the brain and lung. On the other hand, in the septic shock model induced by LPS in rats, there are no studies investigating the effect of either LPS or Nec-1s on the changes in RIPK1, RIPK3, MLKL, and HMGB1 protein expression. In this study, protein expression of RIPK1 in the kidney and lung, RIPK3 in the heart, and MLKL in the kidney was increased 4 hours after LPS administration to rats. It was also observed that there was no change in the HMGB1 protein expression in all tissues of LPS-treated rats. Moreover, Nec-1s did not prevent the LPS-induced increase in the expression of RIPK1, RIPK3, and MLKL proteins in the heart, kidney, and lung tissues. In contrast to the results of studies with Nec-1 [30,57,58], our findings demonstrated that Nec-1s do not affect the LPS-induced increase in the expression of RIPK1, RIPK3, and MLKL proteins in the heart, kidney, and lung tissues. However, these results are consistent with our findings that Nec-1s does not prevent the increase in the expression of RIPK1, RIPK3,

and MLKL proteins measured in the cytosolic and nuclear fractions of TA, RA, PA, and RA isolated 4 hours after LPS administration to rats. Similar to the results of histopathological studies, the expression of RIPK1, RIPK3, MLKL, and/or HMGB1 proteins measured in the tissues of rats administered DMSO or Nec-1s together with saline or LPS was also found to be higher than the values of the control and/or LPS groups. To emphasize once again, according to the results of our *in vivo* studies, while no significant change was observed in the MAP and HR values of rats administered DMSO or Nec-1s with saline compared to the control group, Nec-1s can prevent the hypotension and tachycardia induced by LPS. Therefore, although Nec-1s can prevent LPS-induced hypotension and tachycardia, our findings indicate that systemic administration of DMSO or Nec-1s may lead to enhanced expression of RIPK1, RIPK3, MLKL, and/or HMGB1 proteins in the heart, kidney, brain, and/or lung tissues.

5. Conclusion

The present study revealed for the first time that the inhibition of RIPK1 by Nec-1s prevents the hypotension and tachycardia in response to systemic administration of LPS into rats associated with inflammatory and necroptotic injury in the arterial and vital organs, such as kidney through inhibiting the TLR4/TRIF/RIPK1/RIPK3/MLKL/HMGB1-, TLR4/MyD88/TAK1/IKKβ/NF-κB/iNOS/NO/VASP-, and caspase-8-related pathways. Therefore, Nec-1s may be a potential antihypotensive, antiarrhythmic, antiinflammatory, and antinecroptotic drug candidate in the treatment of inflammatory diseases associated with necroptosis, tissue injury, and organ dysfunction, such as septic shock due to bacterial infections. Regarding the contribution of RIPK1 to the regulation of not only hemodynamic parameters but also necroinflammatory tissue injury, further studies with RIPK1 inhibitors in experimental models of septic shock could provide a novel approach to prevent mortality due to MOF. Importantly, further pharmacological and pharmaceutical studies are also warranted to determine not only the efficacy, but also the toxic effects of Nec-1s will provide benefits to patients with septic shock.

A limitation of this study is that whether Nec-1s exerts its beneficial effects directly by inhibiting the expression and activity of RIPK1 and/or indirectly by decreasing the activity of TLR4/TRIF/RIPK1/RIPK3/MLKL/HMGB1-, TLR4/MyD88/TAK1/IKKβ/NF-κB/iNOS/NO/VASP-, and caspase-8-related pathways in the cardiovascular, renal, cerebral, and pulmonary tissues during LPS-induced septic shock. Therefore, additional experiments need to be conducted in RIPK1 knockout rats to elucidate the molecular mechanisms of the beneficial effects of Nec-1s in the septic shock model. Further detailed experiments at the molecular level are also required to explore the effects of Nec-1s on the interactions between these signaling pathways in the specific cells of cardiovascular, renal, cerebral, and pulmonary tissues expressing RIPK1, such as myocardial, endothelial, vascular, renal tubular, and microglial cells isolated from septic rats. Since animal models provide fundamental information about the mechanism of drug action, pharmacokinetics, and toxicity that other methods cannot replace, animal models remain crucial in developing new therapeutic approaches for septic shock despite several limitations. Hence, considering the critical role of RIPK1-driven necroptosis during endotoxemia, re-evaluation of the effects of Nec-1s in more clinically relevant hyperdynamic and hypodynamic animal models may provide a novel therapeutic target for the treatment of patients with septic shock.

Informed Consent

The authors declare that no humans were used in this study.

Availability of data and material

The data that support the findings of this study are available from the corresponding author upon reasonable request.

Interest of conflict

The authors declare no conflict of interest/competing interests.

Author's contribution

BT conceptualized and conceived the research design, analyzed the data, and drafted the manuscript. BT, SPS, DEY, OB, TK, and MARE carried out the experiments. All authors read and approved the final manuscript.

Funding information

This study was supported by The Scientific and Technological Research Council of Türkiye (TUBITAK) under the Grant Number SBAG-122S479.

References

1. Singer M, Deutschman CS, Seymour CW, Shankar-Hari M, Annane D, Bauer M, Bellomo R, Bernard GR, Chiche JD, Coopersmith CM, Hotchkiss RS, Levy MM, Marshall JC, Martin GS, Opal SM, Rubenfeld GD, van der Poll T, Vincent JL, Angus DC (2016) The Third International Consensus Definitions for Sepsis and Septic Shock (Sepsis-3). JAMA 315:801-810. doi:10.1001/jama.2016.0287
2. Tunctan B, Korkmaz B, Sari AN, Kacan M, Unsal D, Serin MS, Buharalioglu CK, Sahan-Firat S, Schunck WH, Falck JR, Malik KU (2012) A novel treatment strategy for sepsis and septic shock based on the interactions between prostanoids, nitric oxide, and 20-hydroxyeicosatetraenoic acid. Antiinflamm Antiallergy Agents Med Chem 11:121-150. doi:10.2174/187152312803305759
3. Tunctan B, Senol SP, Temiz-Resitoglu M, Guden DS, Sahan-Firat S, Falck JR, Malik KU (2019) Eicosanoids derived from cytochrome P450 pathway of arachidonic acid and inflammatory shock. Prostaglandins Other Lipid Mediat 145:106377. doi:10.1016/j.prostaglandins.2019.106377
4. Zhu Z, Chambers S, Zeng Y, Bhatia M (2022) Gases in sepsis: novel mediators and therapeutic targets. Int J Mol Sci 23:3669. doi:10.3390/ijms23073669
5. Lambden S. Bench to bedside review: therapeutic modulation of nitric oxide in sepsis-an update. Intensive Care Med Exp 7:64. doi:10.1186/s40635-019-0274-x
6. Sandner P (2018) From molecules to patients: exploring the therapeutic role of soluble guanylate cyclase stimulators. Biol Chem 399:679-690. doi:10.1515/hsz-2018-0155
7. Senol SP, Temi M, Guden DS, Cecen C, Sari AN, Sahan-Firat S, Falck JR, Dakarapu R, Malik KU, Tunctan B (2016) Contribution of PPARα/β/γ, AP-1, importin-α3, and RXRα to the protective effect of 5,14-HEDGE, a 20-HETE mimetic, against hypotension, tachycardia, and inflammation in a rat model of septic shock. Inflamm Res 65:367-387. doi:10.1007/s00011-016-0922-5

8. Tunctan B, Korkmaz B, Yildirim H, Tamer L, Atik U, Buharalioglu CK (2005) Increased production of nitric oxide contributes to renal oxidative stress in endotoxemic rat. Am J Infect Dis 1:111-115. doi:10.3844/ajidsp.2005.111.115
9. Tunctan B, Yaghini FA, Estes A, Malik KU (2006) Inhibition by nitric oxide of cytochrome P450 4A activity contributes to endotoxin-induced hypotension in rats. Nitric Oxide 14:51-57. doi:10.1016/j.niox.2005.09.006
10. Tunctan B, Korkmaz B, Dogruer ZN, Tamer L, Atik U, Buharalioglu CK (2007) Inhibition of extracellular signal-regulated kinase (ERK1/2) activity reverses endotoxin-induced hypotension via decreased nitric oxide production in rats. Pharmacol Res 56:56-64. doi:10.1016/j.phrs.2007.03.006
11. Tunctan B, Korkmaz B, Buharalioglu CK, Firat SS, Anjaiah S, Falck J, Roman RJ, Malik KU (2008) A 20-hydroxyeicosatetraenoic acid agonist, N-[20-hydroxyeicosa-5(Z),14(Z)-dienoyl] glycine, opposes the fall in blood pressure and vascular reactivity in endotoxin-treated rats. Shock 30:329-335. doi:10.1097/SHK.0b013e31816471c6
12. Tunctan B, Korkmaz B, Sari AN, Kacan M, Unsal D, Serin MS, Buharalioglu CK, Sahan-Firat S, Cuez T, Schunck WH, Falck JR, Malik KU (2013) 5,14-HEDGE, a 20-HETE mimetic, reverses hypotension and improves survival in a rodent model of septic shock: contribution of soluble epoxide hydrolase, CYP2C23, MEK1/ERK1/2/IKKβ/IκB-α/NF-κB pathway, and proinflammatory cytokine formation. Prostaglandins Other Lipid Mediat 102-103:31-41. doi:10.1016/j.prostaglandins.2013.01.005
13. Tunctan B, Korkmaz B, Sari AN, Kacan M, Unsal D, Serin MS, Buharalioglu CK, Sahan-Firat S, Cuez T, Schunck WH, Manthati VL, Falck JR, Malik KU (2013) Contribution of iNOS/sGC/PKG pathway, COX-2, CYP4A1, and gp91(phox) to the protective effect of 5,14-HEDGE, a 20-HETE mimetic, against vasodilation, hypotension, tachycardia, and inflammation in a rat model of septic shock. Nitric Oxide 33:18-41. 10.1016/j.niox.2013.05.001
14. Tunctan B, Kucukkavruk SP, Temiz-Resitoglu M, Guden DS, Sari AN, Sahan-Firat S (2018) Bexarotene, a selective RXRα agonist, reverses hypotension associated with inflammation and tissue injury in a rat model of septic shock. Inflammation 41:337-355. doi:10.1007/s10753-017-0691-5
15. Tunctan B, Senol SP, Temiz-Resitoglu M, Yilmaz DE, Guden DS, Bahceli O, Horat MF, Sahan-Firat S, Sari AN, Falck JR, Anugu RR, Malik KU (2022) Activation of GPR75 signaling pathway contributes to the effect of a 20-HETE mimetic, 5,14-HEDGE, to prevent hypotensive and tachycardic responses to lipopolysaccharide in a rat model of septic shock. J Cardiovasc Pharmacol 80:276-293. doi:10.1097/FJC.0000000000001265
16. Degterev A, Hitomi J, Germscheid M, Ch'en IL, Korkina O, Teng X, Abbott D, Cuny GD, Yuan C, Wagner G, Hedrick SM, Gerber SA, Lugovskoy A, Yuan J (2008) Identification of RIP1 kinase as a specific cellular target of necrostatins. Nat Chem Biol 4:313-321. doi:10.1038/nchembio.83
17. Newton K, Dugger DL, Wickliffe KE, Kapoor N, de Almagro MC, Vucic D, Komuves L, Ferrando RE, French DM, Webster J, Roose-Girma M, Warming S, Dixit VM (2014). Activity of protein kinase RIPK3 determines whether cells die by necroptosis or apoptosis. Science 343:1357-1360. doi:10.1126/science.1249361
18. Sun L, Wang H, Wang Z, He S, Chen S, Liao D, Wang L, Yan J, Liu W, Lei X, Wang X (2012) Mixed lineage kinase domain-like protein mediates necrosis signaling downstream of RIP3 kinase. Cell 148:213-227. doi:10.1016/j.cell.2011.11.031
19. Udawatte DJ, Rothman AL (2021) Viral suppression of RIPK1-mediated signaling. mBio 12:e0172321. doi:10.1128/mBio.01723-21
20. Wang X, Chai Y, Guo Z, Wang Z, Liao H, Wang Z, Wang Z (2023) A new perspective on the potential application of RIPK1 in the treatment of sepsis. Immunotherapy 15:43-56. doi:10.2217/imt-2022-0219
21. Liu L, Lalaoui N (2021) 25 years of research put RIPK1 in the clinic. Semin Cell Dev Biol 109:86-95. doi:10.1016/j.semcdb.2020.08.007
22. Murphy JM, Czabotar PE, Hildebrand JM, Lucet IS, Zhang JG, Alvarez-Diaz S, Lewis R, Lalaoui N, Metcalf D, Webb AI, Young SN, Varghese LN, Tannahill GM, Hatchell EC, Majewski IJ, Okamoto T, Dobson RC, Hilton DJ, Babon JJ, Nicola NA, Strasser A, Silke J, Alexander WS(2013) The pseudokinase MLKL mediates necroptosis via a molecular switch mechanism. Immunity 39:443-453. doi:10.1016/j.immuni.2013.06.018
23. Pang J, Vince JE (2023) The role of caspase-8 in inflammatory signalling and pyroptotic cell death. Semin Immunol 70:101832. doi:10.1016/j.smim.2023.101832
24. Szobi A, Rajtik T, Adameova A (2016) Effects of necrostatin-1, an inhibitor of necroptosis, and its inactive analogue Nec-1i on basal cardiovascular function. Physiol Res 65:861-865. doi:10.33549/physiolres.933393
25. Jhun J, Lee SH, Kim SY, Ryu J, Kwon JY, Na HS, Jung K, Moon SJ, Cho ML, Min JK (2019) RIPK1 inhibition attenuates experimental autoimmune arthritis via suppression of osteoclastogenesis. J Transl Med 17:84. doi:10.1186/s12967-019-1809-3
26. Takahashi N, Duprez L, Grootjans S, Cauwels A, Nerinckx W, DuHadaway JB, Goossens V, Roelandt R, Van Hauwermeiren F, Libert C, Declercq W, Callewaert N, Prendergast GC, Degterev A, Yuan J, Vandenabeele P (2012) Necrostatin-1 analogues: critical issues on the specificity, activity and in vivo use in experimental disease models. Cell Death Dis 3:e437. doi:10.1038/cddis.2012.176
27. Mohammed S, Nicklas EH, Thadathil N, Selvarani R, Royce GH, Kinter M, Richardson A, Deepa SS (2021) Role of necroptosis in chronic hepatic inflammation and fibrosis in a mouse model of increased oxidative stress. Free Radic Biol Med 164:315-328. doi:10.1016/j.freeradbiomed.2020.12.449
28. Najjar M, Saleh D, Zelic M, Nogusa S, Shah S, Tai A, Finger JN, Polykratis A, Gough PJ, Bertin J, Whalen M, Pasparakis M, Balachandran S, Kelliher M, Poltorak A, Degterev A (2016) RIPK1 and RIPK3 kinases promote cell-death-independent inflammation by toll-like receptor 4. Immunity 45:46-59. doi:10.1016/j.immuni.2016.06.007
29. Nair A, Morsy MA, Jacob S (2018) Dose translation between laboratory animals and human in preclinical and clinical phases of drug development. Drug Dev Res 79:373-382. doi:10.1002/ddr.21461
30. Guan E, Wang Y, Wang C, Zhang R, Zhao Y, Hong J (2017) Necrostatin-1 attenuates lipopolysaccharide-induced acute lung injury in mice. Exp Lung Res 43:378-387. doi:10.1080/01902148.2017.1384083
31. Lan KC, Chao SC, Wu HY, Chiang CL, Wang CC, Liu SH, Weng TI (2017) Salidroside ameliorates sepsis-induced acute lung injury and mortality via downregulating NF-κB and HMGB1 pathways through the upregulation of SIRT1. Sci Rep 7:12026. doi:10.1038/s41598-017-12285-8
32. Dong W, Li Z, Chen Y, Zhang L, Zhang L, Ye Z, Liang H, Li R, Xu L, Zhang B, Liu S, Wang W, Li C, Shi W, Liang X (2018) Necrostatin-1 attenuates sepsis-associated acute kidney injury by promoting autophagosome elimination in renal tubular epithelial cells. Mol Med Rep 17:3194-3199. doi:10.3892/mmr.2017.8214
33. Newton K, Dugger DL, Maltzman A, Greve JM, Hedehus M, Martin-McNulty B, Carano RA, Cao TC, van Bruggen N, Bernstein L, Lee WP, Wu X, DeVoss J, Zhang J, Jeet S, Peng I, McKenzie BS, Roose-Girma M, Caplazi P, Diehl L, Webster JD,

Vucic D (2016) RIPK3 deficiency or catalytically inactive RIPK1 provides greater benefit than MLKL deficiency in mouse models of inflammation and tissue injury. Cell Death Differ 23:1565-1576. doi:10.1038/cdd.2016.46

34. Liu Y, Xu Q, Wang Y, Liang T, Li X, Wang D, Wang X, Zhu H, Xiao K (2021) Necroptosis is active and contributes to intestinal injury in a piglet model with lipopolysaccharide challenge. Cell Death Dis 12:62. doi:10.1038/s41419-020-03365-1
35. Mikus P, Pecher D, Rauova D, Horváth C, Szobi A, Adameová A (2018) Determination of novel highly effective necrostatin Nec-1s in rat plasma by high performance liquid chromatography hyphenated with quadrupole-time-of-flight mass spectrometry. Molecules 23:1946. doi:10.3390/molecules23081946
36. Yoon S, Bogdanov K, Kovalenko A, Wallach D (2016) Necroptosis is preceded by nuclear translocation of the signaling proteins that induce it. Cell Death Differ 23:253-260. doi:10.1038/cdd.2015.92
37. Szobi A, Farkašová-Ledvényiová V, Lichý M, Muráriková M, Čarnická S, Ravingerová T, Adameová A (2018) Cardioprotection of ischaemic preconditioning is associated with inhibition of translocation of MLKL within the plasma membrane. J Cell Mol Med 22:4183-4196. doi:10.1111/jcmm.13697
38. Kearney CJ, Cullen SP, Clancy D, Martin SJ (2014) RIPK1 can function as an inhibitor rather than an initiator of RIPK3-dependent necroptosis. FEBS J 281:4921-4934. doi:10.1111/febs.13034
39. Moriwaki K, Bertin J, Gough PJ, Chan FK (2015) A RIPK3-caspase 8 complex mediates atypical pro-IL-1β processing. J Immunol 194:1938-1944. doi:10.4049/jimmunol.1402167
40. Wang Y, Deng F, Zhong X, Du Y, Fan X, Su H, Pan T (2023) Dulaglutide provides protection against sepsis-induced lung injury in mice by inhibiting inflammation and apoptosis. Eur J Pharmacol 949:175730. doi:10.1016/j.ejphar.2023.175730
41. Carlson D, Willis MS, White DJ, Horton JW, Giroir BP (2005) Tumor necrosis factor-alpha-induced caspase activation mediates endotoxin-related cardiac dysfunction. Crit Care Med 33:1021-1028. doi:10.1097/01.ccm.0000163398.79679.66
42. Asci H, Ozmen O, Erzurumlu Y, Sofu A, Icten P, Kaynak M (2022) Agomelatine protects heart and aorta against lipopolysaccharide-induced cardiovascular toxicity via inhibition of NF-kβ phosphorylation. Drug Chem Toxicol 45:133-142. doi:10.1080/01480545.2019.1663209
43. Mandal P, Feng Y, Lyons JD, Berger SB, Otani S, DeLaney A, Tharp GK, Maner-Smith K, Burd EM, Schaeffer M, Hoffman S, Capriotti C, Roback L, Young CB, Liang Z, Ortlund EA, DiPaolo NC, Bosinger S, Bertin J, Gough PJ, Brodsky IE, Coopersmith CM, Shayakhmetov DM, Mocarski ES (2018) Caspase-8 collaborates with caspase-11 to drive tissue damage and execution of endotoxic shock. Immunity 49:42-55.e6. doi:10.1016/j.immuni.2018.06.011
44. Lemmers B, Salmena L, Bidère N, Su H, Matysiak-Zablocki E, Murakami K, Ohashi PS, Jurisicova A, Lenardo M, Hakem R, Hakem A (2007) Essential role for caspase-8 in toll-like receptors and NFkappaB signaling. J Biol Chem 282:7416-7423. doi:10.1074/jbc.M606721200
45. Simpson DS, Pang J, Weir A, Kong IY, Fritsch M, Rashidi M, Cooney JP, Davidson KC, Speir M, Djajawi TM, Hughes S, Mackiewicz L, Dayton M, Anderton H, Doerflinger M, Deng Y, Huang AS, Conos SA, Tye H, Chow SH, Rahman A, Norton RS, Naderer T, Nicholson SE, Burgio G, Man SM, Groom JR, Herold MJ, Hawkins ED, Lawlor KE, Strasser A, Silke J, Pellegrini M, Kashkar H, Feltham R, Vince JE (2022) Interferon-γ primes macrophages for pathogen ligand-induced killing via a caspase-8 and mitochondrial cell death pathway. Immunity 55:423-441. doi:10.1016/j.immuni.2022.01.003
46. Someda M, Kuroki S, Miyachi H, Tachibana M, Yonehara S (2020) Caspase-8, receptor-interacting protein kinase 1 (RIPK1), and RIPK3 regulate retinoic acid-induced cell differentiation and necroptosis. Cell Death Differ 27:1539-1553. doi:10.1038/s41418-019-0434-2
47. Huang W, Xie W, Gong J, Wang W, Cai S, Huang Q, Chen Z, Liu Y (2020) Heat stress induces RIP1/RIP3-dependent necroptosis through the MAPK, NF-κB, and c-Jun signaling pathways in pulmonary vascular endothelial cells. Biochem Biophys Res Commun 528:206-212. doi:10.1016/j.bbrc.2020.04.150
48. Jones RJ, Jourd'heuil D, Salerno JC, Smith SM, Singer HA (2007) iNOS regulation by calcium/calmodulin-dependent protein kinase II in vascular smooth muscle. Am J Physiol-Heart Circ Physiol 292:H2634-H2642. doi:10.1152/ajpheart.01247.2006
49. Kim HR, Graceffa P, Ferron F, Gallant C, Boczkowska M, Dominguez R, Morgan KG (2010) Actin polymerization in differentiated vascular smooth muscle cells requires vasodilator-stimulated phosphoprotein. Am J Physiol-Cell Physiol 298:C559-C571. doi:10.1152/ajpcell.00431.2009
50. Kopeina GS, Prokhorova EA, Lavrik IN, Zhivotovsky B (2018) Alterations in the nucleocytoplasmic transport in apoptosis: caspases lead the way. Cell Prolif 51:e12467. doi:10.1111/cpr.12467
51. Soriano FG, Guido MC, Barbeiro HV, Caldini EG, Lorigados CB, Nogueira AC (2014) Endotoxemic myocardial dysfunction: subendocardial collagen deposition related to coronary driving pressure. Shock 42:472-479. doi:10.1097/SHK.0000000000000232
52. Korish AA, Arafa MM (2011) Propolis derivatives inhibit the systemic inflammatory response and protect hepatic and neuronal cells in acute septic shock. Braz J Infect Dis 15:332-338
53. Lin B, Jin Z, Chen X, Zhao L, Weng C, Chen B, Tang Y, Lin L (2020) Necrostatin-1 protects mice from acute lung injury by suppressing necroptosis and reactive oxygen species. Mol Med Rep 21:2171-2181. doi:10.3892/mmr.2020.11010
54. Shao RG, Xie QW, Pan LH, Lin F, Qin K, Ming SP, Li JJ, Du XK (2022) Necrostatin-1 attenuates caspase-1-dependent pyroptosis induced by the RIPK1/ZBP1 pathway in ventilator-induced lung injury. Cytokine 157:155950. doi:10.1016/j.cyto.2022.155950
55. Hagiwara S, Iwasaka H, Uchino T, Noguchi T (2008) High mobility group box 1 induces a negative inotropic effect on the left ventricle in an isolated rat heart model of septic shock: a pilot study. Circ J 72:1012-1017. doi:10.1253/circj.72.1012
56. Ren Q, Guo F, Tao S, Huang R, Ma L, Fu P (2020) Flavonoid fisetin alleviates kidney inflammation and apoptosis via inhibiting Src-mediated NF-κB p65 and MAPK signaling pathways in septic AKI mice. Biomed Pharmacother 122:109772. doi:10.1016/j.biopha.2019.109772
57. Liao Z, Ou X, Zhou C, Ma D, Zhao H, Huang H (2022) Xenon attenuated neonatal lipopolysaccharide exposure induced neuronal necroptosis and subsequently improved cognition in juvenile rats. Front Pharmacol 13:1002920. doi:10.3389/fphar.2022.1002920
58. Liao Z, Zhu Q, Huang H (2023) Involvement of IL-1β-mediated necroptosis in neurodevelopment impairment after neonatal sepsis in rats. Int J Mol Sci 24:14693. doi:10.3390/ijms241914693
59. Peek V, Harden LM, Damm J, Aslani F, Leisengang S, Roth J, Gerstberger R, Meurer M, von Köckritz-Blickwede M, Schulz S, Spengler B, Rummel C (2021) LPS primes brain responsiveness to high mobility group box-1 protein. Pharmaceuticals 14:558. doi:10.3390/ph14060558